The Impact of Climate Change on Air Quality–Related Meteorological Conditions in California. Part II: Present versus Future Time Simulation Analysis

ZHAN ZHAO

Department of Land, Air, and Water Resources, University of California, Davis, Davis, and Scripps Institution of Oceanography, University of California, San Diego, La Jolla, California

SHU-HUA CHEN

Department of Land, Air, and Water Resources, University of California, Davis, Davis, California

MICHAEL J. KLEEMAN AND ABDULLAH MAHMUD

Department of Civil and Environmental Engineering, University of California, Davis, Davis, California

(Manuscript received 14 May 2010, in final form 5 October 2010)

ABSTRACT

In this study, the Weather Research and Forecasting (WRF) model was applied to dynamically downscale the Parallel Climate Model (PCM) projection for the climate change impact on regional meteorological conditions in California. Comparisons were made for meteorological fields that strongly influence regional air quality between the current (2000–06) and future (2047–53) downscaling results to infer potential air pollution changes in California. Changes in both the meteorological fields and the implied future air quality vary by region and season. Analyses showed that the normalized number of stagnation days (NNSD) integrating all stagnation events, during which most of the air pollution episodes occur, in California's San Joaquin Valley (SJV) will increase and the intensity of stagnation will be stronger in the future for the two main air pollution seasons (i.e., summer and winter). Increases in surface wind and planetary boundary layer height (PBLH) were observed for the coastal part of Los Angeles County (LAC) during summer, suggesting stronger ventilation in this region. Contrary situations were seen in other parts of the South Coast Air Basin (SoCAB) and SJV. Although a surface wind change was not evident in SJV during winter, there was a significant PBLH decrease. Climate-change-induced variations in surface wind and PBLH were only statistically significant in coastal SoCAB and the southern portion of SJV relative to the corresponding interannual variability; changes in temperature are significant throughout the regions studied. The sea breeze along the coast of California plays an important role in the state's climate and air quality, especially during summertime owing to the stronger intensity compared to wintertime. Analysis of the land–sea temperature contrast and the southwesterly wind along the California coastline indicated that the summertime sea breeze will be stronger in the Central Valley (CV) but weaker for the SoCAB region in the future.

1. Introduction

The Intergovernmental Panel on Climate Change (IPCC) Fourth Assessment Report (Solomon et al. 2007) states that "most of the observed increase in global average temperatures since the mid-20th century is very likely due to the observed increase in anthropogenic greenhouse gas concentrations." Temperature is a decisive meteorological variable for regional climate and air quality. A temperature change can result in a change in atmospheric and oceanic circulations (Nitta and Yamada 1989; Zorita et al. 1992), precipitation (Houghton et al. 2001), extreme weather events (Emanuel 2005), etc. These can lead to air quality changes. Furthermore, temperature is a crucial factor for the formation of some pollutants, such as ozone (Mahmud et al. 2008).

California (CA) is the most populous state in the United States. California's San Joaquin Valley (SJV) is one of the most productive agricultural areas in the world. In addition, several metropolitan cities in CA, such as Los Angeles and San Francisco, are among the

Corresponding author address: Dr. Shu-Hua Chen, Department of Land, Air, and Water Resources, University of California, Davis, One Shields Ave., Davis, CA 95616.
E-mail: shachen@ucdavis.edu

DOI: 10.1175/2010JCLI3850.1

biggest in the United States. California's large agricultural production and population imply high greenhouse gas emissions. Although the per capita greenhouse gas emissions have decreased by about 10% compared to 1990 levels (Next10 2009) as the result of the implementation of control strategies, the overall emissions continue to rise along with population growth in CA. Long-term greenhouse gas emissions may contribute to temperature increase in this region and the surrounding areas through increased radiative forcing, which could in turn affect other meteorological and air quality conditions.

California's regional climate is highly influenced by the Pacific subtropical high (PSH), which normally forms adjacent to the CA coast. The topography of CA is rather diversiform and complex; the coastal regions are under the effect of a cool marine layer caused by PSH and the coastal wind-driven ocean upwelling off the coastline; the Central Valley (CV) is surrounded by mountain ranges, and about 25% of the total surface area in the state is occupied by desert. Because of the geophysical position and intricate topography, together with the aforementioned anthropological factors, CA is likely to be more vulnerable to climate change compared to other regions in the United States (Snyder et al. 2004).

California has been long recognized for its severe summer ozone and winter particulate matter (PM) problems. The concentrations of airborne particles with aerodynamic diameter smaller than 2.5 μm ($PM_{2.5}$) and 10 μm (PM_{10}) consistently exceed both the national and state air quality standards, and the CV is ranked as one of the regions with the highest ground-level ozone concentrations nationwide (Dabdub et al. 1999). Ozone and PMs have serious adverse health effects (Krupnick et al. 1990; Pope et al. 1995; Seaton et al. 1995). Some previous studies highlighted correlations between mortality and fine-particle air pollutants (Dockery et al. 1993), as well as ground-level ozone concentration (Ito et al. 2005; Bell et al. 2004). High PM concentration can also reduce visibility (Eldering and Cass 1996) and influence global climate change (Dickerson et al. 1997), while ozone can damage plants and ecosystems (Fuhrer and Booker 2003). It is essential to explore the potential future changes of these air pollution problems in CA so that adequate control strategies can be established in advance.

Previous studies have investigated potential climate change impacts in the United States using the dynamical downscaling method. Jacobson (2008) studied the effects of agriculture on climate and air quality in CA during August 2006 with a resolution of $0.20° \times 0.15°$ and $0.045° \times 0.05°$ over CA and Los Angeles, respectively, finding a maximum of 2.3-K decrease in August average surface temperature over the CV owing to the irrigation and albedo differences from agriculture. Using the same domain, Jacobson (2010) investigated the climate and air quality response to local CO_2 emissions over CA for two years, as well as over Los Angeles for six months, and concluded that local CO_2 emissions could increase ozone and PM concentration through feedbacks to meteorological fields, such as temperatures, atmospheric stability, winds, precipitation, etc. To the best of our knowledge, the resolution in the Los Angeles domain in these two studies has been the highest resolution applied to this region using the dynamical downscaling method. The results from a chemical transport model in Steiner et al. (2006) suggested that expected climatic changes for temperature and atmospheric humidity in CA could each, individually, lead to a 1%–5% increase in the daily peak ozone in 2050. Caldwell et al. (2009) used the Weather Research and Forecasting (WRF) model to dynamically downscale Community Climate System Model version 3 (CCSM3) data to 12-km resolution to evaluate the downscaling performance in CA. Yet, in their study the greenhouse gas concentrations were fixed at 1990 values and the study only focused on the present climatology. Employing the fifth-generation Penn State–National Center for Atmospheric Research (NCAR) Mesoscale Model (MM5) to downscale the Goddard Institute of Space Studies (GISS) model system, Leung and Gustafson (2005) estimated potential air quality changes over the continental United States based on the future variations of meteorological fields, such as surface temperature (T2), solar radiation, and ventilation. Their results suggested a deterioration of air quality in the western Untied States during fall, while the impact on air quality was not clear for other seasons. MM5 has also been applied to downscale Parallel Climate Model (PCM) simulations (Leung et al. 2004; Liang et al. 2006) to 30–40-km resolutions for current and future climatology, and the results suggested that the downscaling added values with respect to enhancing the small-scale solutions but did not alter the regional mean significantly. Similar conclusions were drawn in Duffy et al. (2006) by comparing the simulation results from four different combinations of regional climate model (RCM) and global climate model (GCM). Other studies (Castro et al. 2005; Rockel et al. 2008) have also suggested that the RCM results are strongly influenced by the driving GCM or reanalysis. Dynamical downscaling adds realistic spatiotemporal details to GCM projections, which is especially obvious over regions with strong mesoscale forcing, associated with topography heterogeneity (Leung et al. 2004; Whetton et al. 2001). The topography in CA is extremely intricate, thus the advantage of dynamical downscaling can be more substantial in this region. However, a high spatial resolution of downscaling is required to replicate the orographic effects and comprehensive mesoscale features for climate studies in CA.

In this paper, the WRF model (Skamarock et al. 2007) is applied to dynamically downscale PCM data to 4-km resolution in CA for both present and future climatology, allowing the future variations of the meteorological conditions to be addressed. The rest of the paper is arranged as follows. The methodology and model configurations are described in section 2. The analysis of results, including stagnation events, future change of air quality–related meteorological variables, and climate change impacts on land–sea breeze are presented in section 3. Remarks and conclusions are given in section 4.

2. Model configurations and methodology

The configuration of the WRF model and the domain setup are identical to those described in Part I of this study (Zhao et al. 2011, hereafter referred to as Part I). The configuration selected in Part I consisted of the Yonsei University (YSU) planetary boundary layer parameterization (PBL) scheme, the Grell–Devenyi cumulus parameterization, WRF single-moment 6-class (WSM6) microphysics, and Rapid Radiation Transfer Model (RRTM) longwave and Dudhia shortwave radiation. The cumulus parameterization scheme was only applied to the outer two domains. It was demonstrated in Part I that, driven by Global Forecasting System (GFS) reanalysis data from the National Centers for Environmental Prediction (NCEP), simulations with this suite of physics schemes reproduce the meteorology conditions in CA for 2000 more accurately than five other combinations of microphysics, cumulus parameterization, and PBL schemes.

The PCM data used in this study are the ''business as usual'' (BAU) scenario simulation B06.44. As described in Part I, the CO_2 level in year 2100 (~710 ppm) represents and approximates a doubling of the level in year 2000 (~371 ppm) (more details about the future scenario forcing applied in PCM BAU B06.44 were described in Dai et al. 2001). This PCM simulation spans a period of approximately one century (1995–2099), which intends to project the trend of climate change in response to increased greenhouse gases and SO_2 instead of actual atmospheric conditions. PCM scenario B06.44 was initialized with atmospheric, land, and sea ice conditions for 1995 obtained from a historical PCM simulation (case B06.28), and ocean conditions for 1995 were derived from the assimilated ocean data (Dai et al. 2004; Pierce et al. 2004). A comprehensive land surface biophysics model (Bonan 1998) was applied in the PCM simulation. The quantitative comparisons between the downscaling results driven by PCM data for a single year (i.e., year 2000 for this case) and actual observations are not meaningful. Therefore, GFS reanalysis data were used during the evaluation for configuration optimization. The simulation results driven by GFS reanalysis were compared to meteorological observations, providing a quantitative evaluation of the model performance. The years from 2000 to 2006 and 2047 to 2053 were chosen to represent the current and future climatology, respectively. An interval of approximately 50 years was taken because PCM has been known to have lower climate sensitivity than other GCMs (Cubasch et al. 2001; Barnett et al. 2001) and the climate change effects on regional meteorology and air quality in CA may not be evident over shorter time intervals. Simulations for two out of every six weeks were conducted, as described in Part I, to span a climatologically relevant period while using a reasonable amount of computational resources. During model simulations driven by PCM data, SST was obtained from the coarse-resolution PCM outputs that were interpolated to the fine-resolution model domain as lower boundary conditions for both the present-day and future simulations. The same vegetation data and soil types from current U.S. Geological Survey (USGS) products were used for both current and future climate simulations. A WRF sensitivity test increasing the CO_2 concentration in the RRTM longwave radiation scheme from 330 to 542.7 ppm to account for the ~1% yr^{-1} CO_2 increase indicated that the greenhouse gas effect is not effective for such short-period (i.e., 17 day) simulation. Thus, the CO_2 increase was not accounted for in the WRF model.

The analysis conducted in Part I showed that PCM data have considerable bias compared to GFS reanalysis data. The comparison of the PCM WRF results (WRF simulations driven by PCM data) and the GFS WRF results (WRF simulations driven by GFS data) with observations indicated that the PCM bias was partially passed to the downscaled WRF results via initial and boundary conditions. It was also demonstrated in Part I that the WRF model has inherent bias relative to observations even when driven by GFS reanalysis. WRF consistently overpredicted regional 10-m wind speed (wsp10) compared to observations, especially during pollution events, and WRF had a systematic warm bias in this region. The model predictions matched surface observations better during summer than the other seasons.

The present versus future simulation comparisons conducted in this paper both use the PCM data–driven WRF results. It is assumed that the PCM bias does not increase with time during the PCM simulation period (1995–2099) and the internal WRF biases are consistent during both present and future years, so that the comparison between present versus future simulations yields a reasonable estimate for climate change impacts on meteorology relevant to air pollution events.

3. Results analysis

a. Stagnation event analysis

Air pollution episodes in CA normally occur during stagnation events, which are mainly characterized by weak winds and low atmospheric planetary boundary layer height (PBLH). Future changes to the total days and the strength of stagnation periods will directly influence future pollutant concentrations. Stagnation events are often associated with dominant high pressure systems, in particular over SJV. Sea level pressure plots are particularly useful indicators of atmospheric stagnation in the SJV. However, the coherence between the sea level pressure field and the stagnation events in SoCAB is unclear, and the appropriate synoptic meteorological features to identify stagnation events over this region are not yet established. Therefore, in this section the stagnation analysis and comparison between present and future climatology focused on SJV only. The future changes of meteorology and consequent air pollution conditions in SoCAB were studied based on 7-yr averages, which are discussed in section 3b. The three criteria to define a stagnation event in the SJV are as follows: 1) a high pressure system, PSH for most cases, intrudes inland and stalls over the region for more than three days; 2) a large magnitude of the sea level pressure gradient (>5 Pa km^{-1}) between the center to the outer edge of the high pressure system; and 3) surface wind speeds (i.e., wsp10) below 3.5 m s^{-1} in the valley. All three criteria must be met to satisfy the stagnation event definition. During the stagnation events, pollutant emissions are trapped below the low boundary layer where weak wind provides very little ventilation, resulting in a steady accumulation of pollutants over time.

As described in Part I, GFS reanalysis data were employed to drive the present seven year WRF simulations as a benchmark to evaluate the WRF downscaling performance driven by PCM data under the same model configurations. Figure 1 shows the 7-yr-averaged normalized number of stagnation days (NNSD) in SJV for each season in the present and future PCM WRF simulations, as well as those from GFS WRF simulations. NNSD was calculated for each season by dividing the total number of days from the stagnation events, which met the three criteria given previously, by the total number of simulated days and then multiplying by the total number of days within that season. This treatment assumed that stagnation days fell randomly throughout each year and that the simulation pattern (2 weeks out

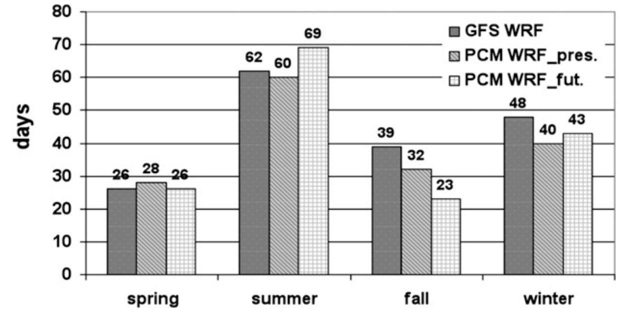

FIG. 1. The NNSD for each season from different WRF simulations: GFS WRF, PCM_WRF_pres. (PCM WRF for 2000–06), and PCM_WRF_fut. (PCM WRF for 2047–53). The values of NNSD are shown above the corresponding bars.

of every 6 weeks) captured an unbiased sampling of those stagnation events. Seasons were defined as spring (=simulation cases 3 and 4, see Part I), summer (=simulation cases 5 and 6), fall (=simulation cases 7 and 8), and winter (=simulation cases 1, 2, and 9). The histograms of ''GFS WRF'' and ''PCM WRF_pres.'' (i.e., GFS WRF and PCM WRF present climate simulations) in Fig. 1 revealed that PCM WRF was inclined to underestimate NNSD for current climate simulations, except for spring. The underestimations from PCM WRF were 3% and 17% for summer and winter, respectively. PCM WRF performed better during spring and summer than fall and winter. The future changes of NNSD (PCM WRF_pres. versus PCM WRF_fut. in Fig. 1) were more significant during summer and fall than spring and winter. This is consistent with the study by Leung and Gustafson (2005), which employed MM5 to dynamically downscale GISS data to the whole continental United States for both present (1995–2005) and future (2045–55) climate. However, this previous study predicted an increased occurrence of stagnation in the future during both summer and fall in most parts of CA, whereas the results from this study predicted a decrease of 28% in the future during fall.

The two main air pollution seasons in the SJV are summer (ozone) and winter (PM). The model results suggested a 15% and 7.5% future increase in the number of stagnation days for summer and winter, respectively. Conversely, the number of spring stagnation days was predicted to decrease by 7%. These results showed favorable circumstances in the future for additional formation of poor air quality conditions during traditional pollution seasons (summer and winter), with reduced air pollution forcing in the spring and fall. Note that the annual number of stagnation days between present and future climate were similar (only one-day difference) but shifted to different seasons, as discussed above.

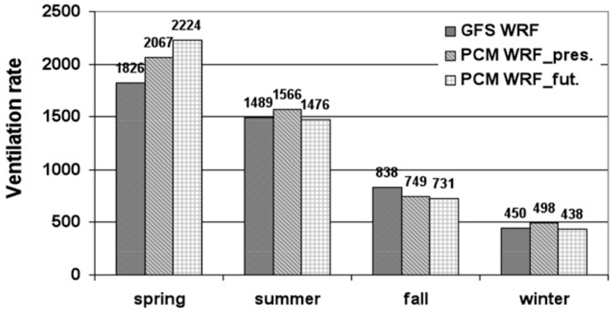

FIG. 2. As in Fig. 1, but for SJV-wide-averaged ventilation rate during the stagnation events. Units are $m^2\ s^{-1}$.

The ''strength'' of a stagnation event can be calculated as the product of the surface wind speed (i.e., wsp10) and PBLH (=total ventilation rate). Ventilation is the main index that determines pollutant concentrations during stagnation events (Kassomenos et al. 1995). Figure 2 shows the regional (SJV-wide) averaged total ventilation rate that was calculated based on all of the stagnation events occurring in each season during the present (2000–06) and future (2047–53) WRF simulations. The comparison of the histograms from GFS WRF and PCM WRF_pres. for current climate simulations indicated weaker stagnations (i.e., larger ventilation rates) from PCM WRF runs, except for during the fall. The PCM WRF simulations overestimated the ventilation rates by 5% and 11% for summer and winter, respectively. In combination with NNSD analysis, this suggested a significant underestimation of the stagnation events from PCM WRF simulations during the two main air pollution seasons, especially during winter. With respect to the impact of future climate change, the total ventilation rate was predicted to decrease for all seasons except for spring. The most significant change of the total ventilation rate (−12%) took place during winter. Driven by the PCM global climate projection, the future decrease of the ventilation rates in summer and winter suggested that future stagnation events would be more severe in SJV. Furthermore, the NNSD of these events during summer and winter were also shown to increase in the future (Fig. 1), indicating negative impacts of future climate change on air quality (i.e., aggravated air pollution problems) in this region during the two main air pollution seasons. Using these WRF-simulated meteorological fields to drive an air quality model [i.e., the University of California, Davis (UCD)–California Institute of Technology (CIT) air quality model], Mahmud et al. (2010) showed that the annual average $PM_{2.5}$ concentration will increase for some areas in SJV in the future.

Compared to GFS WRF, both NNSD and the strength of the stagnations were underestimated from PCM WRF during summer and winter. Furthermore, it was shown in Part I that WRF internally has difficulty capturing the weak winds associated with the stagnations. Both of these indicate that the pollutants will be overventilated in an air quality model driven by the meteorological fields from PCM WRF simulations during the main air pollution seasons. Compared with observations, the present 7-yr (2000–06) annual average $PM_{2.5}$ concentrations were underestimated by about 35%–40% from UCD–CIT air quality model simulation. The results from the air quality model simulation were presented and discussed in Mahmud et al. (2010).

b. Future changes of air quality–related meteorological fields

The climate-induced changes to meteorological variables that affect air quality were explored by comparing the future and present 7-yr averages during the summer and winter seasons. The 7-yr averages for these seasons were calculated for each grid point using the hourly averaged values (Part I) in the analysis domain (i.e., 4-km resolution domain). The spatial distributions of the differences between the future and present averages emphasize how climate change could affect subregions of CA differently.

1) SURFACE WIND ANALYSIS

Figures 3a and 3b illustrate the spatial distribution of the changes in wsp10 (future–present) during summer and winter, respectively. Overall, the changes to wsp10 over most inland regions of CA had opposite signs during the two seasons (i.e., decrease during summer and increase during winter). The regional-averaged change was approximately −3% and 2% during summer and winter, respectively, in SJV, whereas for the SoCAB, future wsp10 was predicted to decrease less than 1% during summer and increase about 3% during winter. Los Angeles County (LAC) is one of the most polluted regions in CA. The average wintertime wsp10 over LAC was shown to increase by approximately 0.5 $m\ s^{-1}$ in the future (Fig. 3b), which is significant when taking into account that the present 7-yr-averaged wintertime wsp10 is about 3–4 $m\ s^{-1}$ in this region (figure not shown). The analysis in Part I showed that the location and strength of the PSH is the crucial large-scale factor that drives the climatology over CA and the adjacent Pacific Ocean. The influence of high pressure systems is more obvious during the summer when the strength of the PSH reaches an annual maximum. The present and future 7-yr-averaged summertime sea level pressure plots of the original PCM data (Fig. 4) indicated a slightly weaker circulation associated with the PSH in the future and consequently weaker northwesterly winds on the right

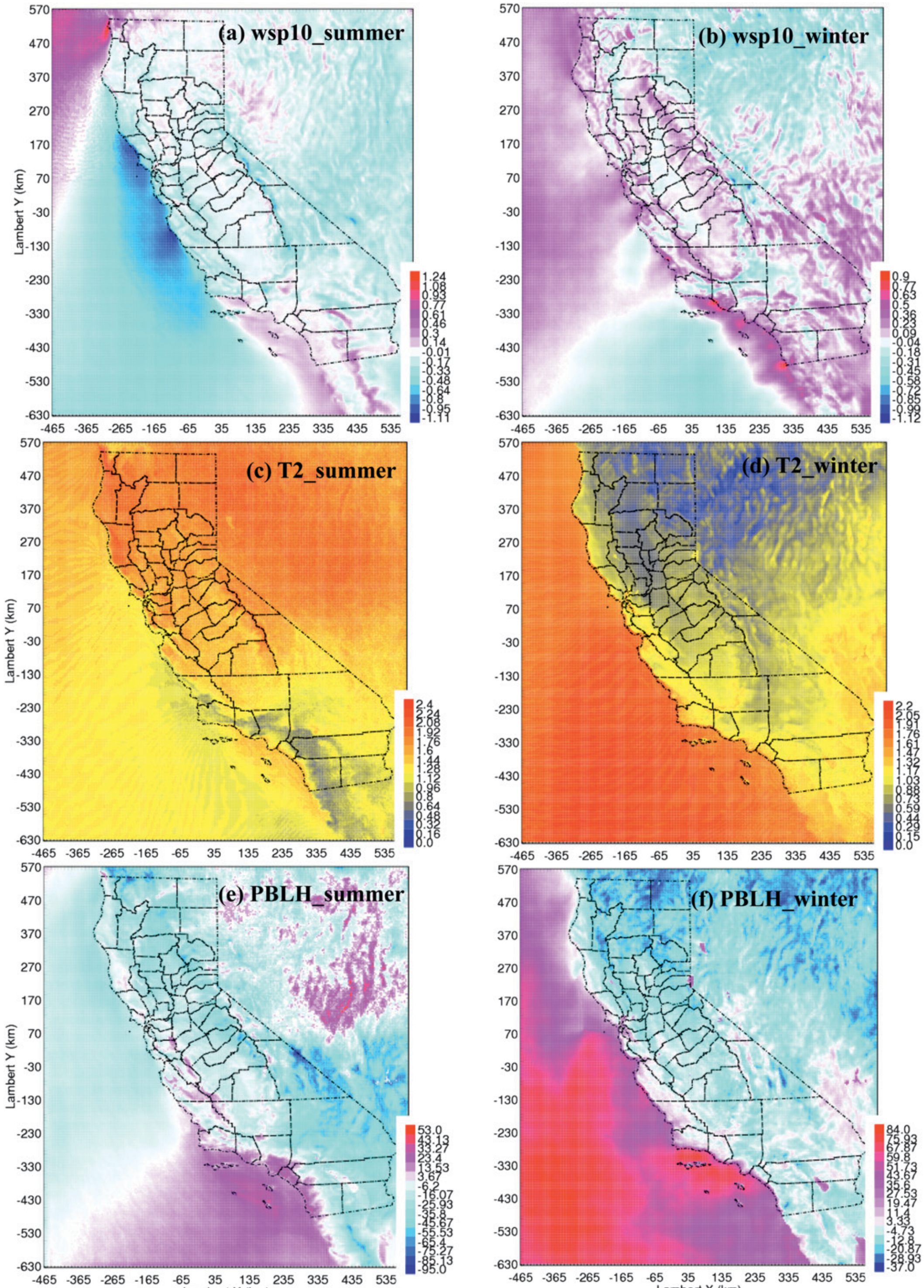

FIG. 3. Predicted change (future − present) in 7-yr-averaged (top) wsp10 (m s^{-1}), (middle) T2 (K), and (bottom) PBLH (m) during (left) summer and (right) winter.

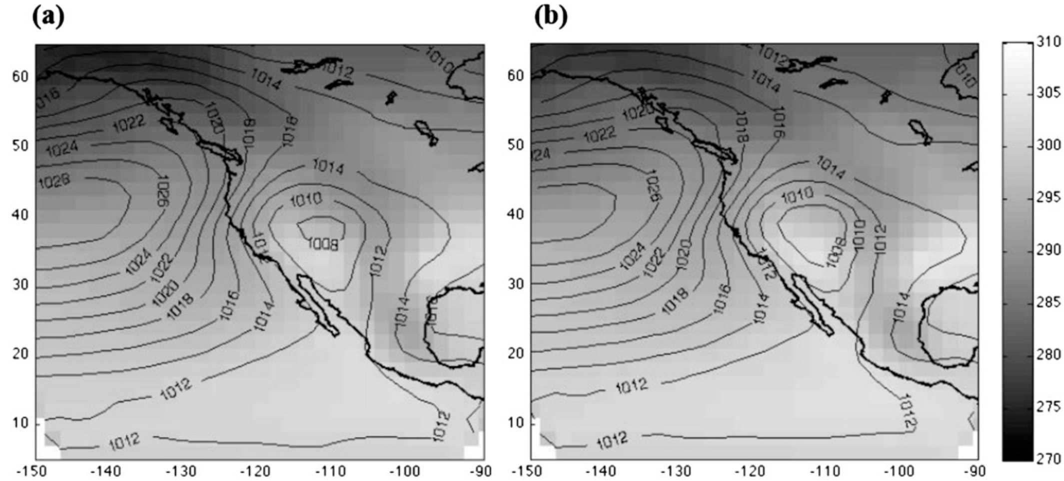

FIG. 4. (a) Present and (b) future 7-yr-averaged summertime surface temperature (shading, K) and sea level pressure (contours, hPa) from PCM.

side of the PSH. This could partially account for the wsp10 decrease over most of the Pacific Ocean within the analysis domain during summer (Fig. 3a). The future change of the wintertime PSH is not as clear. The most obvious summertime wsp10 decrease was along the coastline of northern and central CA (dark blue shown in Fig. 3a), indicating a potential change of the land–sea breeze pattern in this region. More details about the summertime land–sea breeze are explored in section 3c.

2) Surface temperature analysis

The predicted future T2 changes (future–present) from PCM WRF were positive for the whole domain during both summer and winter seasons (Figs. 3c and 3d), and the largest temperature increase of 1.5 ~ 2 K occurred over CA's CV during summertime. The magnitude of the future T2 rise gradually decreased from the northern boundary (over 2 K) to the southern boundary (less than 1 K) for the inland part of the domain during summer (Fig. 3c). An opposite trend was apparent during winter (less than 0.5 K in the north and above 1.3 K in the south; Fig. 3d). In general, the two areas that were predicted to experience the greatest future surface temperature increase during summer (Fig. 5a) were in northwest Canada and the western United States, centered in Nevada. The latter likely contributed to the aforementioned inland summertime north–south trend in T2 change (Fig. 3c). In contrast, this region with maximum future temperature rise in the western United States moved northeast (away from CA) in the wintertime. Furthermore, the magnitude of temperature increase over the Pacific Ocean between 30° and 45°N increased

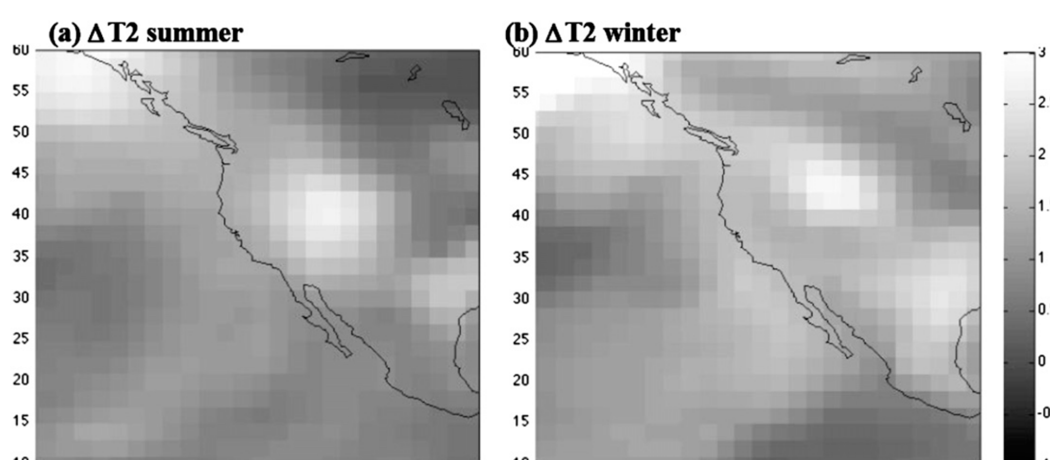

FIG. 5. Predicted change (future − present) in T2 (K) during (a) summer and (b) winter from PCM.

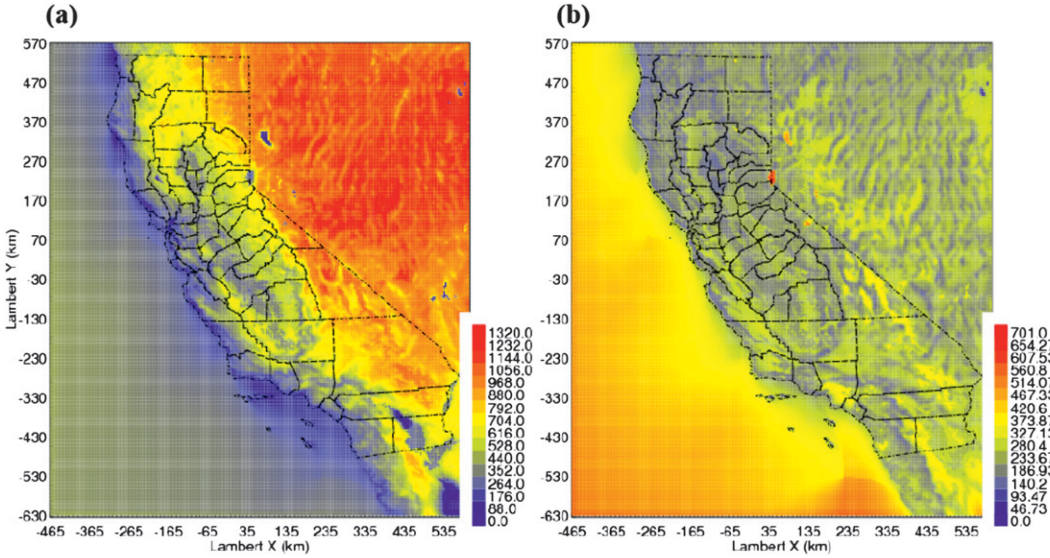

FIG. 6. Present-day 7-yr-averaged (2000–06) PBLH (m) from PCM WRF during (a) summer and (b) winter.

from north to south (Fig. 5b), both of which could contribute to the downscaled wintertime CA regional temperature change trend (Fig. 3d). The much more complex pattern in the downscaled results compared to the driving PCM data (Fig. 5) underlined the necessity for detailed downscaling exercises when evaluating how climate change is expected to influence future meteorology and air quality on regional scales. The pattern of wintertime T2 change (Fig. 3d) was somewhat unexpected. Water has a greater heat capacity than land, and the anthropogenic greenhouse gas emissions that drive global warming are mainly released over land. Therefore, it was anticipated that future temperature increase would be greater over land than over the adjacent ocean. Nevertheless, the opposite trend was observed here during winter (Fig. 3d), with future temperature predicted to increase by approximately 2 K over the ocean but only by less than 1 K over land. A similar pattern was also shown in the original PCM data (Fig. 5b) but to a lesser extent. The large-scale temperature features in PCM (Fig. 5b) may induce greater wintertime cloud cover, humidity, and precipitation over land during the downscaling processes, which may contribute to the enhanced T2 change contrast between ocean and land in PCM WRF simulations relative to the original PCM. The PCM projected summertime T2 rise was around 1.5 K over the inland region of CA and slightly lower over the neighboring Pacific Ocean (Fig. 5a). The large-scale spatial pattern and absolute magnitude of the future summertime temperature variation from WRF simulations (Fig. 3c) matched the original low-resolution PCM data (Fig. 5a). Because of the much finer resolution of the analysis domain and well-resolved topography in the RCM model (WRF in this study), the climate change signal from the downscaling results can be significantly different from the driving GCMs (PCM in this study), particularly in regions with heterogeneous land surface (Whetton et al. 2001; Leung and Ghan 1999). This was evident in the downscaled T2 future variations (Figs. 3c and 3d), which showed much finer features around the coastline and the boundaries of CV compared to the original PCM data (Fig. 5), especially during winter. Both the WRF results and PCM data implied that the temperature contrast between summer and winter seasons in CA would intensify in the future owing to the greater temperature increase over land during summer than during winter. Similar patterns were found in CCM3 data, which were suspected to be the consequence of consistent intraseasonal fluctuations of surface temperature (i.e., T2) and variations in atmospheric water vapor content (Leung and Ghan 1999).

3) PBLH ANALYSIS

Figures 3e and 3f illustrate the spatial distribution of the temporally averaged PBLH difference (future–present) during summer and winter. PBLH is a diagnostic variable in the WRF model that is calculated based on the instability and wind shear of the atmosphere (Hong et al. 2006). PBLH was predicted to decrease during both summer and winter seasons for most inland CA regions. The decrease of 7-yr-averaged PBLH across the entire SJV was 10–30 m during summer and around 10 m during winter. The present-averaged PBLH over SJV was predicted to be approximately 400 m (200 m) during summer (winter) (Fig. 6), thus the future PBLH decreases were approximately 5% for both seasons. Future PBLH was predicted to increase across the Pacific Ocean during winter (Fig. 3f) and across the portion of the Pacific Ocean adjacent to southern CA during summer (Fig. 3e). Strongly affected by the marine boundary layer, PBLH increase was also apparent over coastal regions. Within the marine atmospheric boundary layer (MABL) inversion zone, the average summertime PBLH only reached ~400 m (Fig. 6a) for the coast region of SoCAB. Thus, a 20–30-m increase of the summertime PBLH over this region (Fig. 3e) meant an approximately 7.5% change. Subregions of the SoCAB farther inland were predicted to experience a decrease in PBLH similar to trends predicted for SJV. As mentioned previously in section 3a, stagnation events happen frequently in SJV during summer. Unsurprisingly, the summertime averaged PBLH over inland regions of SoCAB, such as San Bernardino County and the eastern part of Riverside County, was about twice that of the values in SJV (Fig. 6a). Meanwhile, the future PBLH decrease for these inland regions of the SoCAB was roughly double the decrease predicted in the SJV during summer, yielding a similar percentage change in both regions. The current 7-yr-averaged PBLH over the SJV during the winter season was slightly lower than values in the inland SoCAB (Fig. 6b), whereas the predicted future decrease of PBLH was greater over SJV than over inland SoCAB. Therefore, the wintertime PBLH decrease was more significant in SJV. The present 7-yr-averaged PBLH over the ocean was around 400 m during both summer and winter (Fig. 6), so the future PBLH was predicted to increase by roughly 20% over the Pacific Ocean during winter (Fig. 3f). These changes could potentially affect concentrations of pollutants emitted by offshore shipping activities in addition to dimethyl sulfide (DMS) and other precursor species emitted from the coastal ocean waters.

c. Integrated analysis of wind, temperature, and PBLH

Surface wind (i.e., wsp10), temperature (i.e., T2), and PBLH are the three most important meteorological variables directly related to the regional air quality, and they influence air pollutant concentrations simultaneously. Thus, it is necessary to perform an integrated assessment to predict their effects on future air quality. During the summer, the surface wind speed was predicted to increase slightly, and the PBLH was predicted to increase by 7.5% in the coastal region of LAC (CLAC), providing greater ventilation for the summertime pollutants. In contrast, both surface wind and PBLH in SJV were predicted to decease, thus the future atmospheric conditions would be more conducive to the accumulation of summertime pollutants. The correlation between tropospheric ozone concentration and low-level ambient air temperature was shown in some previous studies (Mahmud et al. 2008; Stathopoulou et al. 2008). Thus, the summertime ozone concentration might also be affected by the approximate 2-K future temperature increase in SJV (Fig. 3c). Wsp10 and PBLH are the main meteorological factors that determine wintertime PM concentrations. Predicted future changes to wsp10 were very small in the SJV during winter (Fig. 3b), with some subregions predicted to experience slight increases and others to experience slight decreases. PBLH was predicted to decrease slightly in the SJV (Fig. 3f). These combined trends indicated a slight increase in future wintertime PM concentrations in the SJV. The wsp10 was predicted to increase strongly over most of the SoCAB (Fig. 3b), especially over the coastal regions. PBLH was also predicted to increase over the coastal part of SoCAB, and the decrease of PBLH over the inland part of SoCAB was relatively small. Overall, the ventilation rate was shown to decrease in SJV but increase in SoCAB, particularly over CLAC, during both summer and winter. The qualitative assessments of changes in these meteorological fields and their implications to the change of future air pollutant concentrations are summarized in Table 1. The UCD–CIT air quality model results (Mahmud et al. 2010), which were driven by the meteorological fields from these PCM WRF simulations, confirmed that the annual average airborne particulate matter concentrations increase in some regions of SJV but decrease in CLAC in the future. Note that the discussion of the potential air quality change for the SJV region was based on the whole-season average in this section, thus the conclusions were different from those in the previous section, which were based on the conditions associated with stagnation events.

TABLE 1. Integrated assessment of future changes (I = increase, D = decrease, and II = strong increase) in wsp10, PBLH, and T2, and their potential effects on air pollutant concentration (AQ) in SJV, the coastal region of LAC (CLAC), and SoCAB other than CLAC (SoCABo) during summer and winter.

	Summer				Winter		
Region	WSP10	PBLH	T2	AQ	WSP10	PBLH	AQ
SJV	D	D	I	I	—	D	I
CLAC	I	I	I	D	II	D	D
SoCABo	D	D	I	I	II	D	D

d. Climate change impacts on land–sea breeze

Land–sea breeze (Simpson 1995) is apparent around the coastal regions of CA during periods when the meteorology is not dominated by other strong weather systems. Although the PSH is persistent, especially during summer, and it could affect the climate in CA considerably, the associated synoptic-scale flows are normally weaker than the flows due to surface forcing (i.e., sea breeze and mountain valley wind) (Zhong et al. 2004). The land–sea breeze signal is normally more evident during summer than winter owing to the stronger solar-heating effects, and the nighttime land breeze is typically much weaker than the daytime sea breeze.

Land–sea circulation plays an important role in the meteorology and air quality in CA. The sea breeze in Southern CA follows a classical pattern similar to that described by Kitada (1987), Novitsky et al. (1992), and Koo and Reible (1995). The cool marine surface air and the pollutants emitted from the coastal region of SoCAB move inland with a penetration distance that depends on the land–sea temperature contrast. This influx of cool marine air reduces the daytime temperature near the ground, leading to the establishment of a temperature inversion (cold air trapped beneath warmer air aloft), which inhibits vertical mixing in the atmosphere and traps pollutant emissions within the shallow mixing layer. In contrast, the nighttime land breeze may transport these pollutants back out over the ocean in an elevated layer of warmer air that stays aloft in the land breeze front (a convergence zone). This recycled plume may return onshore during the afternoon of the next day, affecting the pollutant concentrations near the surface. In general, the land–sea breeze potentially reduces the net ventilation by trapping pollutants close to the surface within the coastal zone of SoCAB. The effect of the sea breeze around the Bay Area is quite different. The analysis in section 3a showed that stagnation events occur frequently during the summer in the CV, and pollutants accumulate close to the emissions' source owing to a lack of ventilation. The sea breeze in the Bay Area transports the marine air and emissions from San Francisco into the CV through the Carquinez Strait and separates into a northward flow toward the Sacramento Valley and a southward flow toward the SJV as it impinges against the Sierra Nevada Mountains located on the eastern side of the CV (Bao et al. 2008). These marine air flows transport pollutant emissions between regions within the valley, and they reduce the surface temperature and increase the humidity of air in the valley at the same time. A more stable condition is expected because of the decreased surface temperature. The nighttime return flow back toward the ocean is very weak in the CV owing to the complex topography and flow patterns in this region. Although the land–sea breeze could change the spatial distribution of the pollutant concentrations in the valley, the net effect of the sea breeze on air quality in the CV is not yet clear. The future change of the summertime land–sea breeze system could potentially influence the climate and air quality in both the CV and the coastal part of SoCAB.

The strength of the land–sea breeze is directly proportional to the land–sea temperature contrast, which reaches its peak around 1400–1500 local time (LT) before the net warming effect of the solar radiation becomes negative. Figures 7a and 7b show the predicted future changes of summertime T2 at 1400 and 0200 LT over CA. The 1400 LT T2 increase in the Sacramento Valley, which is in the northern part of the CV, was greater than the increase over the neighboring Pacific Ocean, at the same latitude, by approximately 0.5 K. The increased land–sea temperature contrast would produce a stronger sea breeze in this region, transporting more coastal and marine air into the CV, and consequently change the meteorological and air quality conditions in this region. In Southern CA, the 1400 LT T2 increase was only ~0.7 K in the coastal region, while the temperature increase over the adjacent ocean was ~1.5 K, which suggested a future decrease of land–sea temperature contrast and less marine air flowing into the SoCAB during the summer. The pattern of predicted future T2 variation at 0200 LT (Fig. 7b) was quite similar to the pattern predicted at 1400 LT (Fig. 7a) in Northern CA, but the effect on the land breeze would be the reverse. Higher nighttime temperatures over land weaken the land breeze rather than strengthen it. The predicted T2 change over inland and ocean regions at 0200 LT in Southern CA suggested a slight strengthening of the predicted land breeze in this region. The weaker daytime sea breeze and stronger nighttime land breeze in Southern CA implied that more polluted inland air would be brought over the ocean at night, while fewer residual plumes over the ocean would move inland during the day. Therefore, the future change of the land–sea circulation may lead to a decrease of the summertime pollutant concentration in SoCAB, especially over the coastal regions.

The direction of the land–sea breeze is perpendicular to the coastline, which is approximately aligned in the northwest-to-southeast direction (45°) around both the Bay Area (gateway to the CV) and Southern CA. The sea breeze therefore flows approximately from the southwest direction (i.e., southwesterly wind), while the land breeze flows approximately from the northeast direction (i.e., northeasterly wind) in both regions. The 7-yr-averaged southwesterly component of the wind at 1400 0200 was calculated for each grid point during the summer season. Positive (negative) values of the southwesterly component correspond to sea (land) breeze. The formula used to calculate the southwesterly wind component was $U\sin(45°) + V\cos(45°)$, where U is the x component of the 10-m wind, and V is the y component

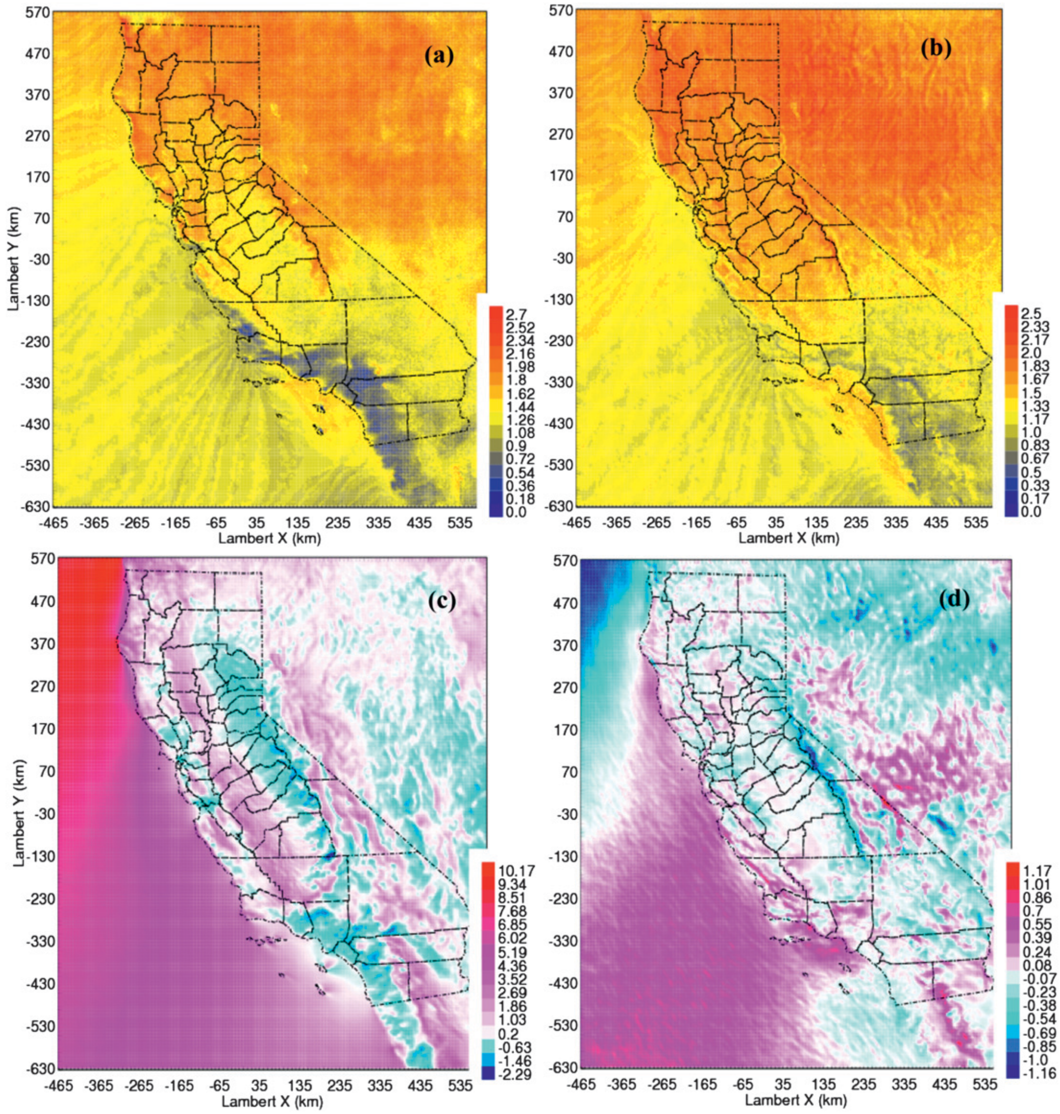

FIG. 7. Spatial distribution of future change (future − present) for T2 (K) at (a) 1400 and (b) 0200 LT. The 10-m southwesterly wind component (m s^{-1}) at (c) 1400 and (d) 0200 LT during summer.

of the 10-m wind. Figures 7c and 7d depict the future change of the southwesterly wind component at 1400 and 0200 LT during summer. The southwesterly increase in the CV (Fig. 7c) was likely due to the marine flows with southwesterly momentum entering the valley through the Carquinez Strait. By contrast, a future sea breeze decrease was predicted in the coastal region of Southern CA (Fig. 7c). The predicted sea breeze behaved as expected based on the predicted land–sea temperature contrasts in these two regions. The predicted nighttime southwesterly flows (Fig. 7d) slightly increased for the coastal part of Southern CA; therefore, the land breeze (northeasterly signified by a negative value) was predicted to slightly decrease in the coastal part of SoCAB. The opposite was predicted for the Bay Area and the CV. The predicted future changes to the sea breeze were much larger than to the land breeze (Fig. 7c versus 7d), which is attributed to the strength difference between the land and sea breeze.

e. Significance test

The comparison between the present versus future meteorology was complicated by the natural variation within each 7-yr interval. Large amounts of interannual variability can make it impossible to discern the effects of climate change with reasonable confidence. In the present study, a *p*-value analysis (Fig. 8) was performed

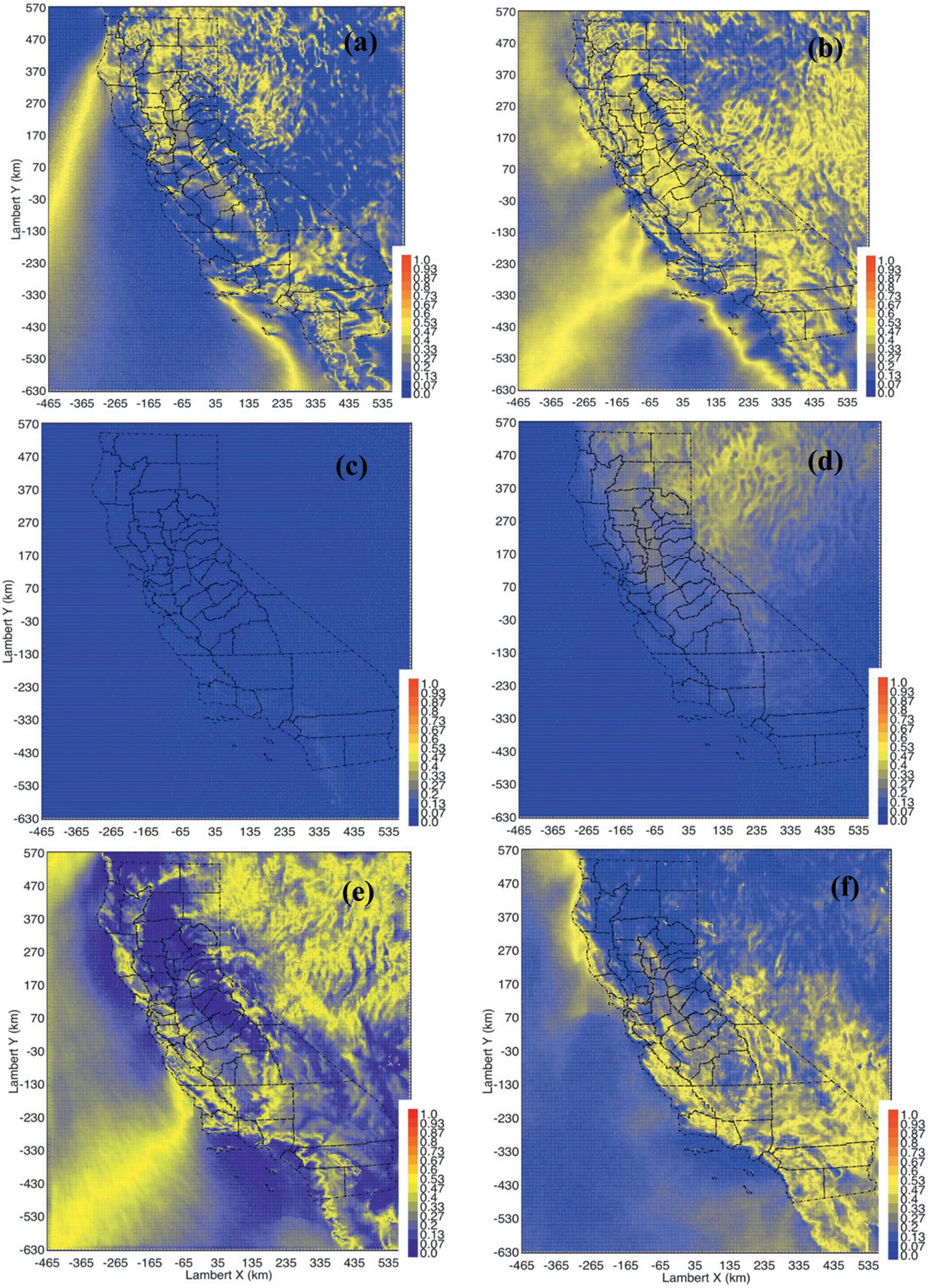

FIG. 8. Corresponding p values of the plots in Fig. 3. The p value quantifies the likelihood that present (2000–06) meteorological conditions will occur in the future (2047–53) due to climate change. Note that smaller p values represent bigger climate change signals.

to evaluate the significance of the climate change (i.e., the trend between current and future climate; i.e., Fig. 3) compared to the interannual variability. The *p* value was calculated based on the annual mean and variance of meteorological data from each 7-yr interval in both present (2000–06) and future (2047–53) time periods using the Student's *t* distribution with 12 degrees of freedom. A small *p* value indicated that the climate change signals were stronger than the interannual variability, while a large *p* value indicated that climate change might have a relatively small impact on the variable of interest (Mahmud et al. 2010). Normal thresholds for statistical significance require *p* values smaller than 0.1 (90% confidence) or 0.05 (95% confidence). The highest confidence results (lowest *p* values) in Fig. 8 were those associated with temperature, suggesting that the predicted increases in surface temperature were statistically significant at the 95% confidence level relative to interannual variability. This pattern was expected considering the ~1% yr^ -1 increase of greenhouse gases concentrations in the driving PCM data. The *p* values calculated for wsp10 and PBLH were higher, with no broad region experiencing future changes that were statistically significant at the 95% confidence level. This was not surprising considering the high nonlinearity of the atmosphere and lack of a direct relationship between temperature increase (due to greenhouse gases) and wind–PBLH changes, which were more or less related to temperature gradient changes. Changes to wsp10 were significant in the southern portion of the SJV (summer only) and in the coastal portion of the SoCAB (summer and winter). Overall, the *p* values for T2, wsp10, and PBLH were smaller during summer than winter in CA, suggesting the climate change was likely to be more statistically significant during summer.

4. Remarks and conclusions

In this paper, the present and future climatology in CA were simulated by dynamical downscaling the global PCM data with a BAU scenario to a spatial resolution of 4 km over a span of 14 years (2000–06 in the present and 2047–53 in the future). All findings in this study are based on the assumption that the PCM future projections are a somewhat accurate representation of a future climate. Downscaling to such fine resolution was essential to characterize the intricate mesoscale features in CA, which are induced by complex topography. The spatial resolution used in this study is much finer than previous CA climate studies that used a comparable time window. The changes in the predicted future meteorology have direct implications for air pollution in two of the most polluted air basins in the United States—the SJV and the SoCAB.

Current air pollution episodes in the SJV and the SoCAB usually occur during stagnation events characterized by weak surface wind and low PBLH. The pollutants are trapped within the boundary layer with concentrations increasing over time until the episode dissipates. Both NNSD, which reflects the accumulated days of all the stagnation events, and the strength of the stagnation events in SJV were underestimated from the downscaling results driven by PCM data relative to the benchmark simulations driven by GFS reanalysis data. Compared to the current climate, NNSD in SJV was predicted to increase during both summer (15%) and winter (7.5%) in 2050. The strength of the stagnation events (inversely proportional to the regional ventilation rate) was predicted to increase during all seasons except for spring. The combination of these changes to NNSD and strength of the stagnation events indicated that air pollution problems in the SJV would likely worsen in the future. Detailed air quality modeling results for CA driven by the meteorological fields from the PCM WRF simulation in this study indicate that the extreme stagnation events in the future climate lead to higher surface airborne particulate matter concentrations compared to extreme events in the current climate. The reduced wind speed during extreme pollution events traps pollutants close to their emissions sources. Urban populations are therefore exposed to higher concentrations of sources located close to urban centers (diesel engines), but they experience lower concentrations of distant sources (shipping, rail) (Mahmud et al. 2010, submitted to *Environ. Sci. Technol.*).

Future changes in terms of wsp10, T2, and PBLH were calculated for the two main air pollution seasons (i.e., summer and winter) throughout the 7-yr window. In the CLAC, both the wsp10 and PBLH were predicted to increase, while T2 was predicted to remain relatively unchanged during summer. These factors would provide more ventilation for the summertime pollutants in this region. The situation was reversed in both the inland portions of the SoCAB and the SJV, yielding a favorable meteorological condition for pollutant accumulation during summer. The wintertime change was less obvious and somewhat uncertain, and the analysis of the wsp10 and PBLH indicated a slightly weaker (stronger) ventilation rate in the SJV (SoCAB) in the future. Using air quality models, Mahmud et al. (2010) presented a rigorous analysis regarding the future air quality, especially with respect to fine airborne particulate matter (i.e., $PM_{2.5}$), in CA due to climate change impacts.

Confidence intervals calculated for the change to meteorological variables between 2000–06 and 2047–53 indicated that the temperature increase was statistically significant ($p < 0.05$), but changes to wsp10 and PBLH were only statistically significant ($p < 0.1$) in some portions of SoCAB and SJV, whereas, for other regions, the interannual variability within the time periods 2000–06 and 2047–53 appeared to be larger than the climate change signal in 50 years for wsp10 and PBLH. Results also suggested that the climate change signal was more significant during summer than winter in CA.

The land–sea breeze in the coastal regions of CA plays a significant role in the meteorology and air quality conditions in these areas. The sea breeze brings the marine air, coastal emissions, and residual plumes from previous days inland and transports pollutant emissions between subregions of CA during the day. At the same time, the increased surface wind due to the sea breeze is offset by the associated temperature inversion induced by the influx of cool marine air. The future increase (decrease) of summertime land–sea temperature contrast, which is the dominant factor for the development of a land–sea breeze, in northern (southern) CA at 1400 LT implied a stronger (weaker) sea breeze intruding into the CV (SoCAB). The situation was reversed at 0200 LT, so that the nighttime land breeze was predicted to be weaker (stronger) around the Bay Area (SoCAB) in the future. Analysis of the land–sea breeze speed (southwesterly component of the 10-m wind around the coastal regions) confirmed that the sea breeze increase (decrease) around the Bay Area (coastal region of SoCAB).

Acknowledgments. This research was supported by the California Air Resources Board under Contract 04-349. We gratefully acknowledge the U.S. Department of Energy's (DOE) Office of Science (BER) Accelerated Climate Prediction Initiative (ACPI) project for supplying PCM model simulations. We thank Dr. Dan Cayan and Mary Tyree at the Scripps Institution of Oceanography, University of California, San Diego. Thanks also go to the National Typhoon and Flood Research Institute and National Central University, Taiwan, which provided computer clusters for part of the model simulations.

REFERENCES

Bao, J. W., S. A. Michelson, P. O. G. Persson, I. V. Djalalova, and J. M. Wilczak, 2008: Observed and WRF-simulated low level winds in a high-ozone episode during the Central California Ozone Study. *J. Appl. Meteor. Climatol.,* **47,** 2372–2394.

Barnett, T. P., D. W. Pierce, and R. Schnur, 2001: Detection of anthropogenic climate change in the world's oceans. *Science,* **292,** 270–274.

Bell, M. L., A. McDermott, S. L. Zeger, J. M. Samet, and F. Dominici, 2004: Ozone and short-term mortality in 95 US urban communities, 1987–2000. *J. Amer. Med. Assoc.,* **292,** 2372–2378.

Bonan, G., 1998: The land surface climatology of the NCAR Land Surface Model (LSM 1.0) coupled to the NCAR Community Climate Model (CCM3). *J. Climate,* **11,** 1307–1326.

Caldwell, P., H. N. S. Chin, D. C. Bader, and G. Bala, 2009: Evaluation of a WRF dynamical downscaling simulation over California. *Climatic Change,* **95,** 499–521.

Castro, C. L., R. A. Pielke Sr., and G. Leoncini, 2005: Dynamical downscaling: Assessment of value retained and added using the Regional Atmospheric Modeling System (RAMS). *J. Geophys. Res.,* **110,** D05108, doi:10.1029/2004JD004721.

Cubasch, U., and Coauthors, 2001: Projections of future climate change. *Climate Change 2001: The Scientific Basis,* J. T. Houghton et al., Eds., Cambridge University Press, 525–582.

Dabdub, D., L. L. DeHaan, and J. H. Seinfeld, 1999: Analysis of ozone in the San Joaquin Valley of California. *Atmos. Environ.,* **33,** 2501–2514.

Dai, A., T. M. L. Wigley, B. A. Boville, J. T. Kiehl, and L. E. Buja, 2001: Climates of the twentieth and twenty-first centuries simulated by the NCAR climate system model. *J. Climate,* **14,** 485–519.

——, W. M. Washington, G. A. Meehl, T. W. Bettge, and W. G. Strand, 2004: The ACPI climate change simulations. *Climatic Change,* **62,** 29–43.

Dickerson, R. R., S. Kondragunta, G. Stenchikov, K. L. Civerolo, B. Doddridge, and B. N. Holben, 1997: The impact of aerosols on solar ultraviolet radiation and photochemical smog. *Science,* **278,** 827–830.

Dockery, W. D., and Coauthors, 1993: An association between air pollution and mortality in six US cities. *N. Engl. J. Med.,* **329,** 1753–1759.

Duffy, P. B., and Coauthors, 2006: Simulations of present and future climates in the western United States with four nested regional climate models. *J. Climate,* **19,** 873–895.

Eldering, A., and G. R. Cass, 1996: Source-oriented model for air pollutant effects on visibility. *J. Geophys. Res.,* **101,** 19 343–19 369.

Emanuel, K., 2005: Increasing destructiveness of tropical cyclones over the past 30 years. *Nature,* **436,** 686–688, doi:10.1038/nature03906.

Fuhrer, J., and F. Booker, 2003: Ecological issues related to ozone: Agricultural issues. *Environ. Int.,* **29,** 141–154.

Hong, S.-Y., Y. Noh, and J. Dudhia, 2006: A new vertical diffusion package with an explicit treatment of entrainment processes. *Mon. Wea. Rev.,* **134,** 2318–2341.

Houghton, J. T., Y. Ding, D. J. Griggs, M. Noguer, P. J. van der Linden, X. Dai, K. Maskell, and C. A. Johnson, Eds., 2001: *Climate Change 2001: The Scientific Basis*. Cambridge University Press, 944 pp.

Ito, K., S. F. De Leon, and M. Lippmann, 2005: Associations between ozone and daily mortality: Analysis and meta-analysis. *Epidemiology,* **4,** 446–457.

Jacobson, M. Z., 2008: Short-term effects of agriculture on air pollution and climate in California. *J. Geophys. Res.,* **113,** D23101, doi:10.1029/2008JD010689.

——, 2010: The enhancement of local air pollution by urban CO_2 domes. *Environ. Sci. Technol.,* **44,** 2497–2502, doi:10.1021/es903018m.

Kassomenos, P., V. Kotroni, and G. Kallos, 1995: Analysis of climatological and air quality observations from greater Athensarea. *Atmos. Environ.,* **29,** 3671–3688.

Kitada, T., 1987: Turbulence structure of sea breeze front and its implication in air pollution transport—Application of k–ε turbulence model. *Bound.-Layer Meteor.,* **41,** 217–239.

Koo, Y., and D. D. Reible, 1995: Flow and transport modeling in the sea breeze. Part II: Flow model application and pollutant transport. *Bound.-Layer Meteor.,* **76,** 209–234.

Krupnick, A. J., W. Harrington, and B. Ostro, 1990: Ambient ozone and acute health effects: Evidence from daily data. *J. Environ. Econ. Manage.,* **18,** 1–18.

Leung, L. R., and S. Ghan, 1999: Pacific Northwest climate sensitivity simulated by a regional climate model driven by a GCM. Part II: $2 \times CO_2$ simulations. *J. Climate,* **12,** 2031–2053.

——, and W. I. Gustafson Jr., 2005: Potential climate change and implications to U.S. air quality. *Geophys. Res. Lett.,* **32,** L16711, doi:10.1029/2005GL022911.

——, Y. Qian, X. Bian, W. M. Washington, J. Han, and J. O. Roads, 2004: Mid-century ensemble regional climate change scenarios for the western United States. *Climatic Change,* **62,** 75–113.

Liang, X.-Z., J. Pan, J. Zhu, K. E. Kunkel, J. X. L. Wang, and A. Dai, 2006: Regional climate model downscaling of the U.S. summer climate and future change. *J. Geophys. Res.,* **111,** D10108, doi:10.1029/2005JD006685.

Mahmud, A., M. Tyree, D. Cayan, N. Motallebi, and M. J. Kleeman, 2008: Statistical downscaling of climate change impacts on ozone concentrations in California. *J. Geophys. Res.,* **113,** D21103, doi:10.1029/2007JD009534.

——, M. Hixson, J.-L. Hu, Z. Zhao, S.-H. Chen, and M. J. Kleeman, 2010: Climate impact on airborne particulate matter concentrations in California using seven year analysis periods. *Atmos. Chem. Phys. Discuss.,* **10,** 11 097–11 114.

Next10, cited 2009. California Green Innovation Index. [Available online at http://www.nextten.org/pdf/GII/Next10_GII_2009.pdf.]

Nitta, T., and S. Yamada, 1989: Recent warming of tropical sea surface temperature and its relationship to the Northern Hemisphere circulation. *J. Meteor. Soc. Japan,* **67,** 375–383.

Novitsky, M., D. D. Reible, and B. M. Corripio, 1992: Modeling the dynamics of the land-sea breeze circulation for air quality modeling. *Bound.-Layer Meteor.,* **59,** 163–175.

Pierce, D. W., T. P. Barnett, R. Tokmakian, A. Semtner, M. Maltrud, J. Lysne, and A. Craig, 2004: The ACPI Project, element 1: Initializing a coupled climate model from observed conditions. *Climate Change,* **62,** 13–28.

Pope, C. A., III, D. V. Bates, and M. E. Raizenne, 1995: Health effects of particulate air pollution: Time for reassessment. *Environ. Health Perspect.,* **103,** 472–480.

Rockel, B., C. L. Castro, R. A. Pielke Sr., H. Von Storch, and G. Leoncini, 2008: Dynamical downscaling: Assessment of model system dependent retained and added variability for two different regional climate models. *J. Geophys. Res.,* **113,** D21107, doi:10.1029/2007JD009461.

Seaton, A., W. MacNee, K. Donaldson, and D. Godden, 1995: Particulate air pollution and acute health effects. *Lancet,* **345,** 176–178.

Simpson, J. E., 1995: *Sea-Breeze and Local Winds*. Cambridge University Press, 234 pp.

Skamarock, W. C., J. B. Klemp, J. Dudhia, D. O. Gill, D. M. Barker, W. Wang, and J. G. Powers, 2007: A description of the advanced research WRF version 2. NCAR Tech. Note NCAR/TN-468+STR, 88 pp.

Snyder, M. A., L. C. Sloan, and J. L. Bell, 2004: Modeled regional climate change in the hydrologic regions of California: A CO2 sensitivity study. *J. Amer. Water Resour. Assoc.,* **40,** 591–601.

Solomon, S., D. Qin, M. Manning, Z. Chen, M. Marquis, K. B. Averyl, M. Tignor, and H. L. Miller, Eds., 2007: *Climate Change 2007: The Physical Science Basis*. Cambridge University Press, 996 pp.

Stathopoulou, E., G. Mihalakakou, M. Santamouris, and H. S. Bagiorgas, 2008: Impact of temperature on tropospheric ozone concentration levels in urban environments. *J. Earth Syst. Sci.,* **117,** 227–236.

Steiner, A. L., S. Tonse, R. C. Cohen, A. H. Goldstein, and R. A. Harley, 2006: Influence of future climate and emissions on regional air quality in California. *J. Geophys. Res.,* **111,** D18303, doi:10.1029/2005JD006935.

Whetton, P. H., J. J. Katzfey, K. J. Hennesey, X. Wu, J. L. McGregor, and K. Nguyen, 2001: Using regional climate models to develop fine resolution scenarios of climate change: An example for Victoria, Australia. *Climate Res.,* **16,** 181–201.

Zhao, Z., S.-H. Chen, M. J. Kleeman, M. Tyree, and D. Cayan, 2011: The impact of climate change on air quality–related meteorological conditions in California. Part I: Present time simulation analysis. *J. Climate,* in press.

Zhong, S., C. D. Whiteman, and X. Bian, 2004: Diurnal evolution of three-dimensional wind and temperature structure in California's central valley. *J. Appl. Meteor.,* **43,** 1679–1699.

Zorita, E., V. Kharin, and H. Von Storch, 1992: The atmospheric circulation and sea surface temperature in the North Atlantic area in winter, their interaction and relevance for Iberian precipitation. *J. Climate,* **5,** 1097–1108.